**Supplementary Material**
The supplementary material contains 8 figures, three movies, and additional experimental procedures.

**Figure S1. Probability of bout type across grating speeds (refers to Figure 1).**
In these plots of rostral bend amplitude vs, head yaw, we see the probability of a bout falling within that parameter space across all grating speeds tested, from 0 to 40 mm/s. We can see the slow (lower left) cluster shift, and the emergence of the fast (top right) beginning at 12.5 mm/s and increasing in intensity as faster grating speeds are shown.

**Figure S2. Method of bout categorization and clustering (refers to Figure 2).**
We divided all bouts into groups by setting a fixed threshold based on kinematic parameters. We calculated this threshold (dotted line) by fitting a binormal function to the fast trial pool distribution of the rostral bend amplitude and calculating the minimum between the two maximums of the distribution. We observed that bouts with high rostral bend amplitude are correlated with high bout speeds (fast bouts) while bouts with low values of amplitude normally have slow bout speeds (slow bouts). This principle applies to separating forward bouts from turns as well.

**Figure S3. Behavioral effects of laser ablation on different neuronal populations plotted against grating speed (refers to Figure 4).**
Larvae were recorded swimming to different speeds of OMR gratings before and after laser ablation of specific populations: either (A) nMLF neurons, (B) RoM neurons, or (C) both Mauthner cells. Pre-ablation data is plotted in grey for each group and post-ablation data is plotted in color for the average bout parameters: bout speed (mm/s), maximum tail-beat frequency (Hz), bout duration (ms), and bout distance (mm). Larvae with nMLF neurons ablated: n= 17 larvae, 1506 pre bouts, 860 post bouts. Larvae with RoM neurons ablated: n= 7 larvae, 771 pre bouts, 569 post bouts. Larvae with both Mauthner cells ablated: n= 3 larvae, 593 pre bouts, 443 post bouts. Error bars are the standard error of the mean. (D) To assess the damage caused to surrounding cells during the laser ablation procedure, we backfilled reticulospinal neurons with texas-red dextran (red) in transgenic larvae expressing GCaMP5G panneuronally (green) (Ahrens, Orger, Robson, Li, and Keller. *Nat. Methods.* 2013). These GCaMP expressing neurons are known to fluoresce for an extended period when damaged. We found very minimal and localized damage sites surrounding successful ablation of single neurons (n= 3 larvae). Scale bar is 20 µm.

**Figure S4. Effect of stimulation pipette proximity on locomotor and nMLF calcium responses (refers to Figure 5).**
(A) Reference image including Texas Red Dextran-labeled nMLF cells and location of the stimulation pipette (red dashed line). Note that the pipette tip is almost touching the bright cell at the left edge of the nMLF (generally outlined by black dashed line). Scale bar is 50 µm. (B) Reference image for a pipette tip at a remote location from the same larva as in A, same scale. (C) Number of bouts elicited in two seconds of stimulation plotted against pipette distance from the edge of the original cell of stimulation. (D) Peak Δf/f in two seconds of stimulation plotted against pipette distance from the edge of the original cell of stimulation**.** n= 10 larvae which contributed to data on all panels.

**Figure S5. Electrophysiology reveals nMLF large cell firing increases with grating speed (refers to Figure 6).**
(A) Bright-field and fluorescent image of the nMLF neurons. Arrow indicates the pipette's location, white dotted line approximates the midline. Rostral is at the top of the image. (B)

Example trace of a targeted loose-patch recording from a right MeLr nMLF cell. Each trial recorded voltage over 27 seconds, with grating motion initiated at 9 s and returning to static at 18 s (red dotted lines). This example was recorded during 15mm/s grating speed. (C) Enlargement of two individual spikes from trace shown in B. (D) Raster-gram of a single cell for 60 consecutive trials, red dotted lines indicate initiation and ceasing of grating motion (moving at 15 mm/s for these trials). (E) Average time until the first spike is recorded following initiation of grating motion (n=11 larvae) vs. grating speed for all four speeds tested. Error bars are the standard error of the mean. (F) Filtered instantaneous firing rate averaged over 11 larvae (approximately 745 trials per speed). Blue trace represents 3 mm/s, green = 7.5 mm/s, orange = 15 mm/s, red = 30 mm/s with red dotted lines indicating initiation and cessation of grating motion.

**Figure S6. Correction of motion artifact during calcium imaging and methods of determining significance (refers to Figure 7).**
(A) Top: Motion correction applied to individual frames acquired during imaging a single z-plane (864 frames, two minutes, Experimental procedures). Bottom shows zoomed in version between the two dashed red lines in the top graph. Two different metrics for motion correction are shown: in black we see distance moved from previous frame, whereas in red we see distance moved from the average frame in the plane. The vertical dashed blue lines correspond to the frames shown below in B. (B) Eight images showing the frames acquired while imaging the plane shown in A above. The anatomy is the sum of all the frames in the plane and is used as the reference to align all the frames acquired in this plane to. The following seven images show individual frames. The pre-alignment frame (green) is shown superimposed with the post-alignment frame (magenta). (C) Calcium responses in the four large nMLF cell types triggered on four different behaviors: swim bouts, swim bouts which transition into struggles, turns, and struggles (the fraction of all swim bouts accounted for by each individual behavior is shown as a percentage +/- S.E.M.). The behavior y-axis of 100 degrees cumulative tail angle applies to all behavioral traces except the struggle, which is 200 degrees. The average motion correction traces accompanying the calcium responses are alongside in red. (D) For each scatter plot in Figure 7 $(x_i, y_i)$ {i=1,...,n, where n is the total number of swim bouts performed while the cell was being imaged} we computed 1000 controls by randomly permuting the y coordinates: $(x_i, \text{permute}(y_i))$, performing linear regression on each control and then plotted a histogram of the R-squared values of the controls. A correlation was deemed significant if its R-squared value was higher than the 95-th percentile of the R-squared values of its associated 1000 controls. The four histograms shown here correspond to the four cells shown in Figure 7F.

**Figures S7. The calcium activity observed in nMLF cells coincides with locomotor output even in a paralyzed fictive preparation (refers to Figure 7).**
In this experiment, large identifiable nMLF cells loaded with calcium green dextran were imaged in paralyzed larvae where ventral root activity was recorded as a read out of fictive locomotion. (A) Top: Calcium activity recorded from two nMLF neurons, both MeM cells, morphology shown at right. Middle: Smoothed and filtered firing rate of ventral root output. Bottom: Power (maximum-minimum) calculated from raw ventral root recording. Red asterisk marks the ventral root bout expanded at right. Red asterisk on bout trace represents burst expanded above. In all three panels red-dotted lines mark the time of grating motion. (B) Left: Histogram of recorded spikes from ventral root recordings across all trials (30 ms bins, n = 4 larvae and 28 trials). Right: Average $\Delta F/F$ response from those same trials separated by cell type (left and right identifiable cells were pooled by cell type. MeLr in red (n=35), MeLc in blue (n=38), MeLm in green (n=7), and MeM cells in black (n=12)). Note that during each trial bouts did not always occur at the same points during the trial, however, on average one can observe the most consistent response immediately following the start of grating motion. Each trial was treated

independently, rather than averaged by larva, since the number of trials was limited due to the technical difficulty of the experiment.

**Figure S8. Imaging of retinal ganglion cell projections alongside reticulospinal neurons shows no evidence of direct connections (refers to Figure 8).**
Transgenic larvae expressing a green fluorescent protein (Dendra) under a driver for retinal ganglion cells (Ath5) via the Gal4/UAS expression system were injected with texas-red dextran to label reticulospinal cells and then imaged at high resolution by two-photon microscopy. (A) Shows a wide view of the head, with the auto-fluorescence in the eyes visible as yellow at the top of the image. Skin auto-fluorescence is also visible, mostly in the green channel. Rostral is at the top, scale bar is 50 µm. (B) A more detailed view, the images move sequentially from dorsal to ventral with the z-position listed in µm on each individual panel. The majority of the retinal ganglion cell projections are dorsal to the position of the nMLF and its dendrites. Rostral is at the top, scale bar is 20 µm. Ath5:Gal4;UAS:Dendra larvae were a generous gift from Dr. Filippo Del Bene, Institut Curie. UAS:Dendra was the same construct used in Arrenberg, Del Bene, and Baier, *PNAS*, 2009.

**Movie S1. Fast bouts vs. slow bouts**
Movie showing a sample fast bout (red) and a sample slow bout (blue) as reconstructed from the freely swimming behavioral tracking data.

**Movie S2. Large nMLF neurons labeled in a reticulospinal stack**
Movie is an image stack of reticulospinal neurons backfilled with dextran with pseudocolored labels overlayed with the large nMLF neurons discussed in this paper. The movie is moving from dorsal to ventral, and the play-rate is 10 Hz.

**Movie S3. Head-restrained swimming during *in vivo* two-photon calcium imaging**
Movie showing a larva's behavior during 40 seconds of an imaging experiment (4X real-time). The stimulus shown is represented by the moving grating below: four 10 s periods of a grating moving at 0, 10, 0 and 5 mm/s respectively. The image is taken from below such that the circular object in the background corresponds to the objective. The laser can be seen scanning over the head of the larva.

**Supplementary Experimental Procedures**
Free-swimming behavioral assay
Behavior was recorded from above at 700 Hz using an IR-sensitive, high-speed camera (MC1362, Mikrotron), fitted with a machine vision lens (Schneider apo-Xenoplan 2.0/24) and a 790 nm long pass filter. Larvae were illuminated from below by a 20 x 10 cm LED backlight (850 nm, Nerlite). The gratings were projected onto a 150 mm x 150 mm opal glass diffuser 5 mm below the larva using a DLP projector (BenQ). During trials, if a larva failed to reach the opposite end during the recording period, a 10 mm/s grating was displayed until it swam the remaining distance. Following background subtraction and inversion, the image was smoothed with a two-dimensional spatial boxcar filter, and the global maximum determined. This point always lies approximately between the larva’s eyes. This point was then used to seed a flood fill on a thresholded version of the image, and the center of mass of the resulting shape which defines a consistent location on the larva's head, was defined as the larva's location. The direction of the tail was found by finding the maximum pixel value on a 0.65 mm diameter circle around this point, which corresponded roughly to the position of the swim bladder. To evaluate tail curvature we successively computed the angles of seven tail segments 0.39 mm long, by finding the center of mass of the pixel values along an arc centered on the end of the previous segment. Tail curvature was measured by summing the absolute deviation from the body angle

at the head at all points along the tail. This measure was used to find the start and end of individual bouts. A custom-made script written in Matlab 2010 (Mathworks) was used to compute the kinematic parameters online. The angle of the last segment is used to count the number of oscillations of each bout and measure the tail-beat frequency as the inverse of the time between successive extreme tail positions in the same direction. The rostral bend amplitude was measured as the maximum peak-to-peak bend amplitude 1.17 mm caudal to the swim bladder in our analysis. The head yaw is defined as the maximum peak-to-peak amplitude of the angle of a line between the swim bladder and a point between the two eyes of the larva during each forward bout. Detected bouts with one cycle of oscillation or less were excluded.

Spinal injections

Larvae four to seven dpf were anaesthetized with 0.02% Tricaine (MS-222, Sigma) and pressure injected with either a 10% solution of calcium green dextran (10,000 MW, Invitrogen) in water or 10% solution of Texas Red dextran (3,000 MW, Invitrogen) in water into axons in the spinal cord to retrogradely label reticulospinal cell somas as described previously ((Huang et al., 2013; O'Malley et al., 1996; Orger et al., 2008). Larvae were given one or more days to recover in E3 medium following injection. All experiments requiring injection were performed on AB WT larvae homozygous for the nacre mutation (*mitfa* -/-) which reduces melanophore pigmentation throughout the skin but not eyes, making imaging more permissible without compromising visual function.

Custom built two-photon microscope with projected visual stimulus

The custom built two-photon microscope used a Mai Tai HP Ti-Sapphire laser tuned to 950 nm. The visual stimulus consisted of a square OMR grating of period 10 mm. It was projected, using an amber (590 nm) LED mounted into a miniature LCOS projector, onto an opal glass screen directly underneath the larva. Stimulus light was filtered with a narrow band-pass filter, and there was no detectable stimulus bleed-through.

Two-photon imaging of nMLF cells in paralyzed larvae

Stacks were taken of the nMLF consisting of 40 planes with 2 μm separation, and each plane was imaged for 200 seconds at 7.23 frames per second using a quad-interlaced scan pattern that ensured that each cell was sampled evenly at four times this frame rate. The visual stimulus shown during the 200 seconds per plane consisted of 10 trials of moving gratings, each lasting 10 seconds, with 10 seconds of static gratings in between trials. The trials were always shown in the same order for ease of analysis. These stacks were analyzed using software custom written in Matlab (Mathworks). The software allows users to select the same cell in different planes and then computes the fluorescence traces for the cell (the full three-dimensional region of interest or ROI) for the full 1440 frames that includes the 10 presentations of moving gratings and the 10 periods of static gratings. The baseline fluorescence for the cell was calculated as the average fluorescence for the whole ROI across frames when the static grating was presented.

Two-photon imaging of nMLF cells in paralyzed larvae with accompanying fictive recordings of motor output

Nacre -/- AB larvae were injected with calcium green dextran as above at 5 dpf. At 7 dpf, larvae were prepared for experiments by mounting in low-melting temperature agarose, injected with 1 mM α-bungarotoxin (Tocris), and an access window was cut out of the agarose on the right side of the body from the swim bladder to the anal pore. During recordings, intact larvae were placed under 20x magnification and a recording electrode was positioned in contact with the side of the body while a gentle suction was applied. Trials consisted of 10 seconds of baseline recording, 10 seconds of grating motion, and 10 seconds following motion during imaging in a single plane

at 6 Hz. Ventral root recordings were made with borosilicate glass pipettes (resistance 0.5-1 mΩ) sucked onto the muscle at the myotomal border, filled with external solution pH 7.7 (Drapeau et al., 1999). Data were acquired in current mode using Clampex 10.3.14 software (Molecular Devices) AC 300 Hz, Gain 500, Bessel 2.2 kHz. Custom microscope and imaging software provided by Intelligent Imaging Innovations, Inc. (3i, Denver, CO) including a Mai Tai Deepsee laser (Spectra-Physics) tuned to 950 nm and a Zeiss Axio Examiner Z1 with a Zeiss W Plan-APO 20x water-immersion objective. Gratings were presented using an MP160 pocket projector (3M) filtered with a Wratten #29 (Kodak). The stimulus was created using Labview 2012 (National Instruments) and delivered as above except presentation was on the left side of the animal rather than underneath. Data were analyzed using custom software in Matlab (Mathworks, Natick, MA).

# SUPPLEMENTAL FIGURE 1

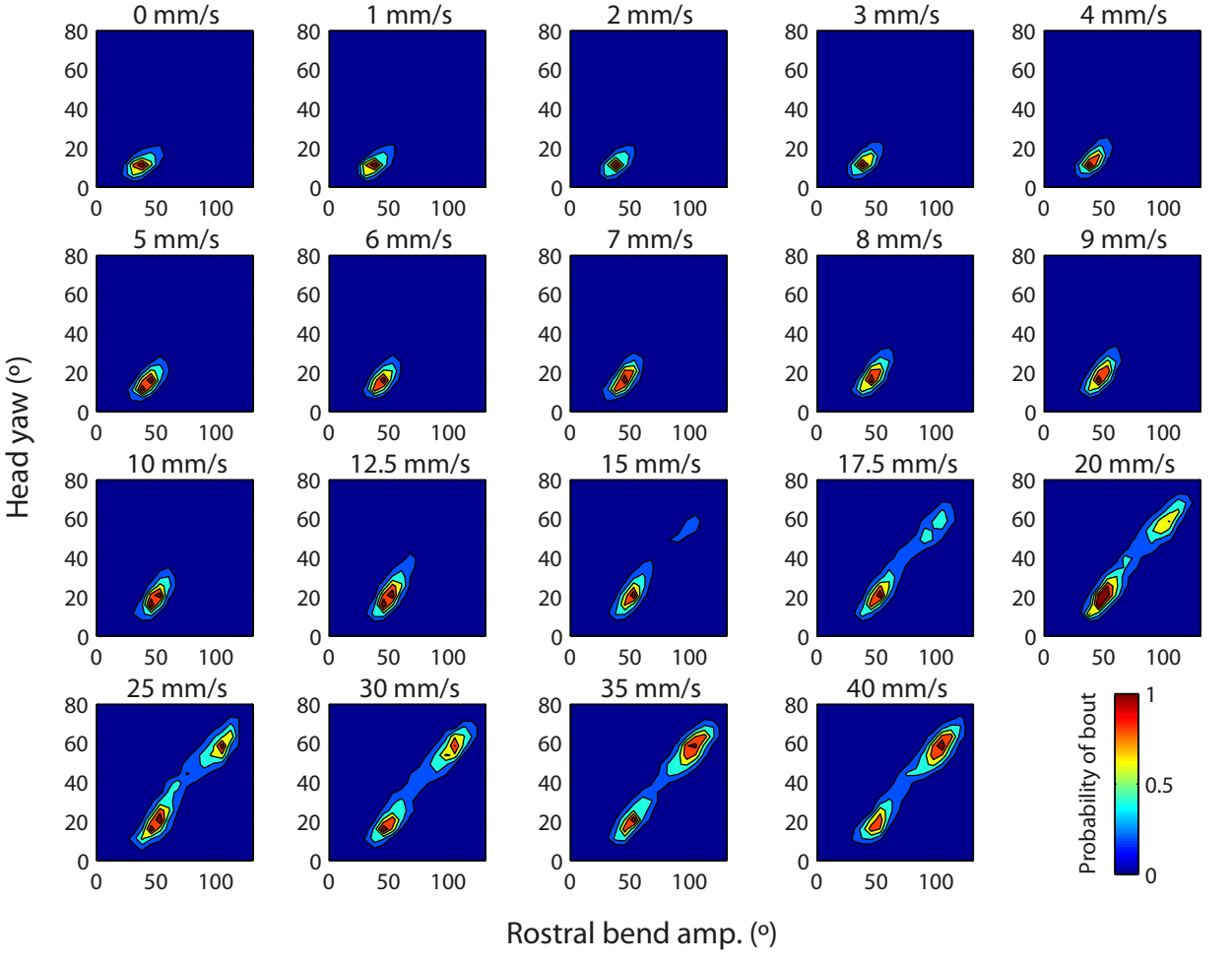

# SUPPLEMENTAL FIGURE 2

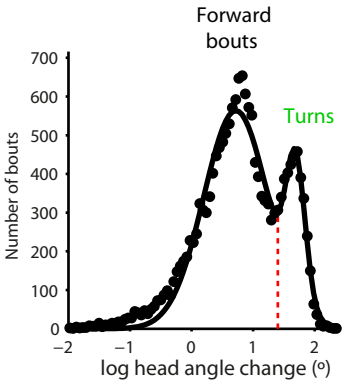


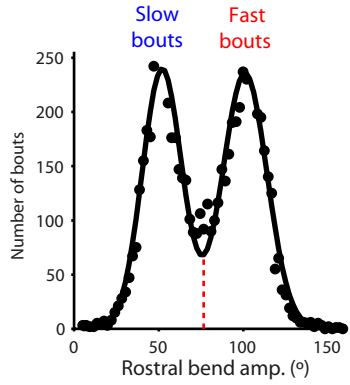


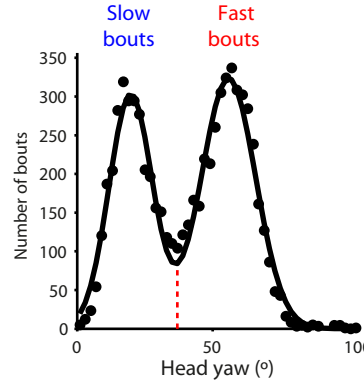


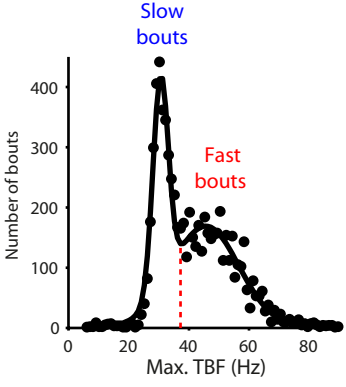


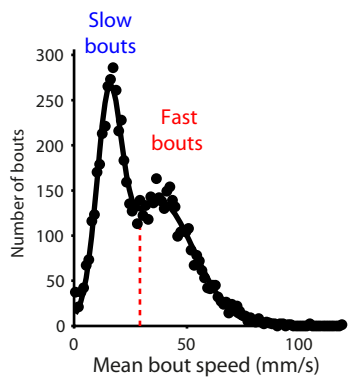

# SUPPLEMENTAL FIGURE 3

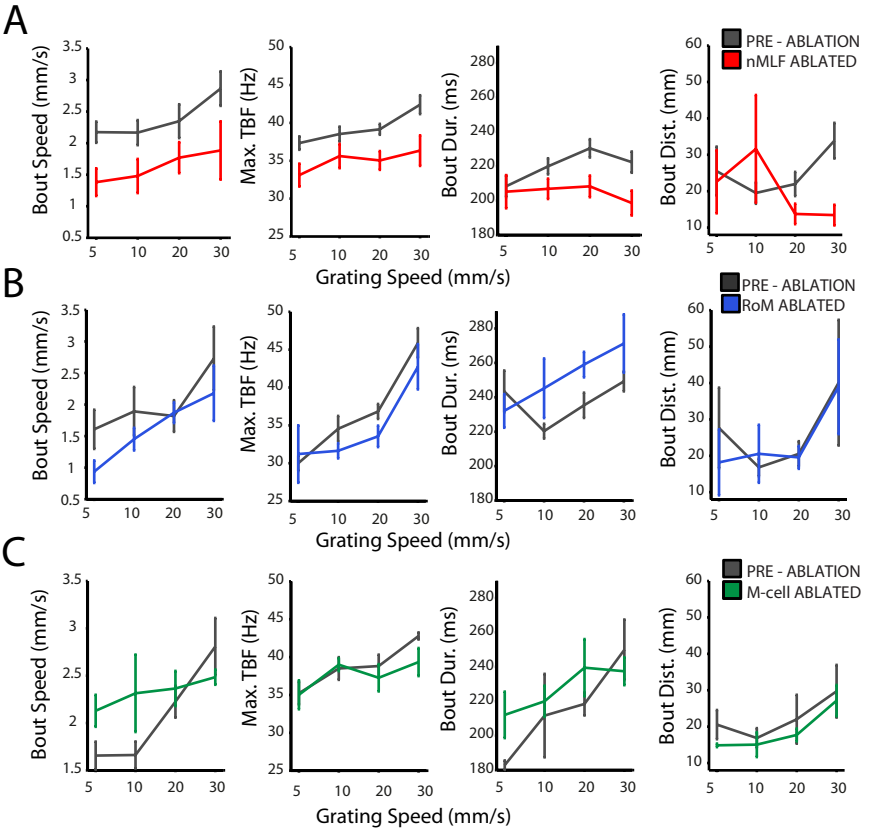


D

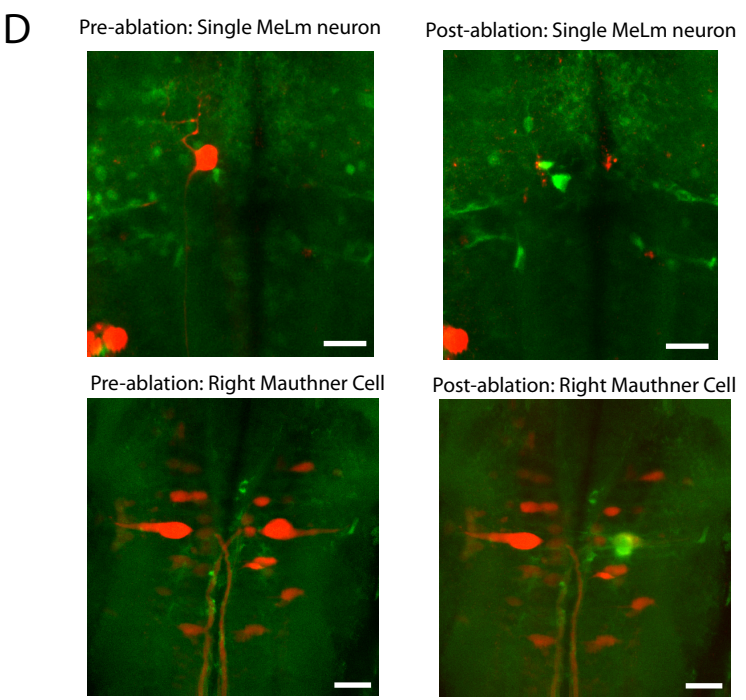

# SUPPLEMENTAL FIGURE 4

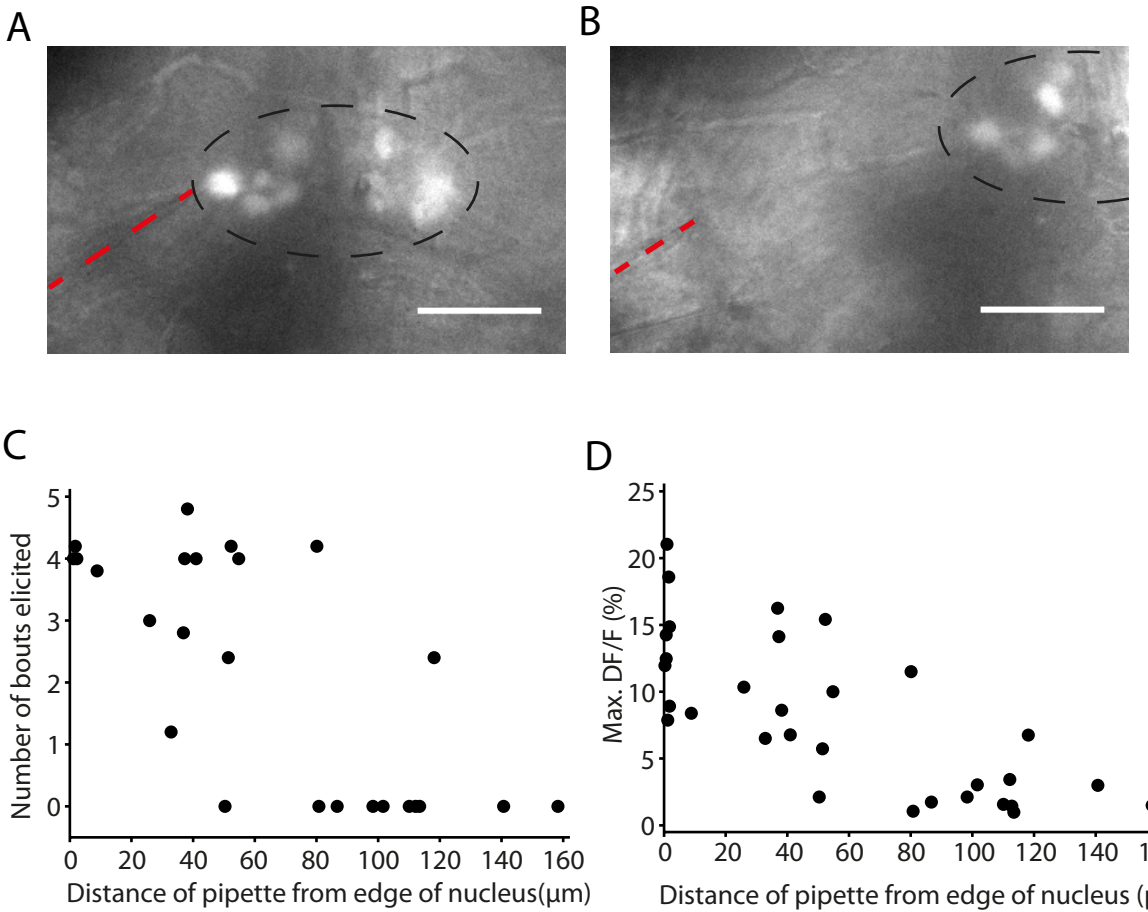

# SUPPLEMENTAL FIGURE 5

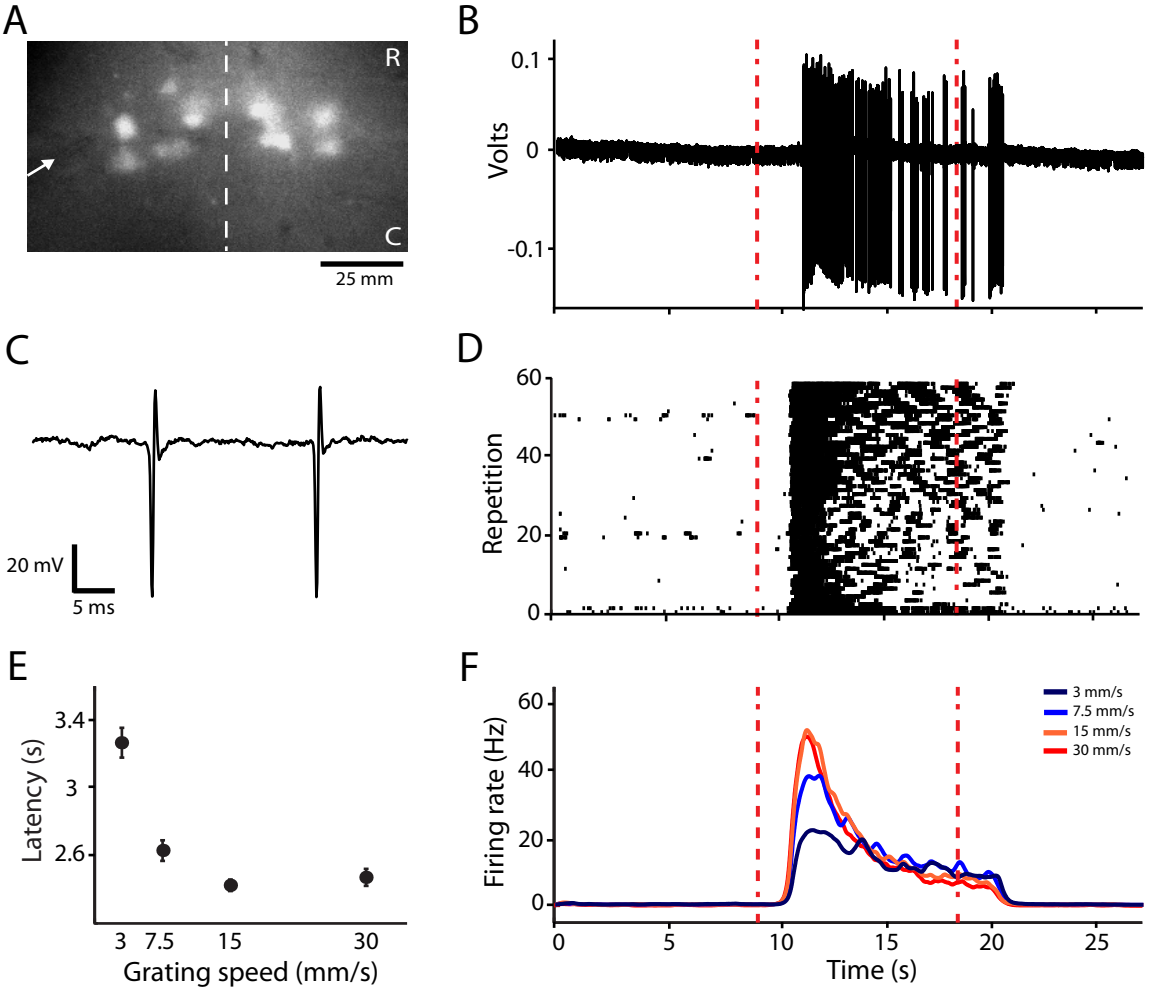

# SUPPLEMENTAL FIGURE 6

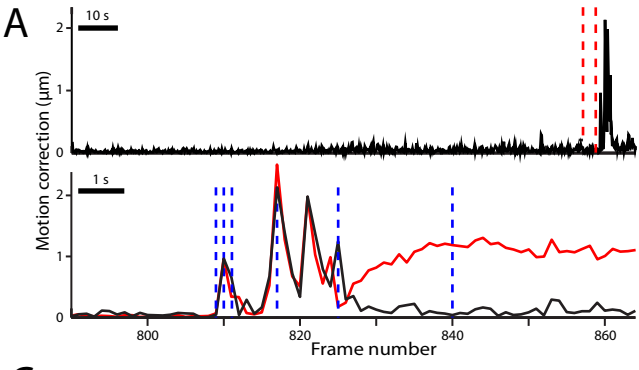


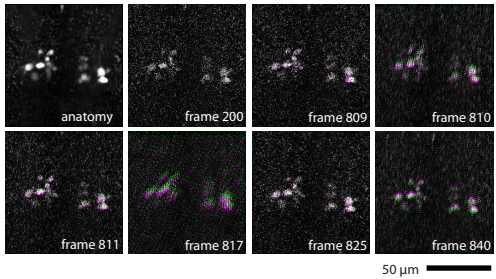


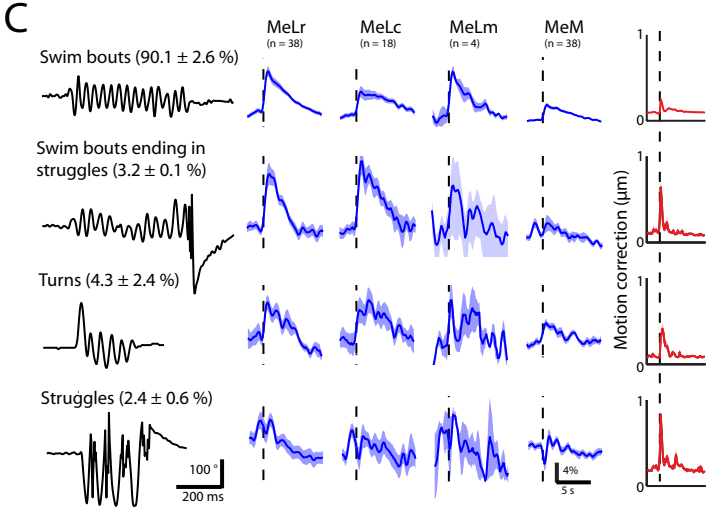


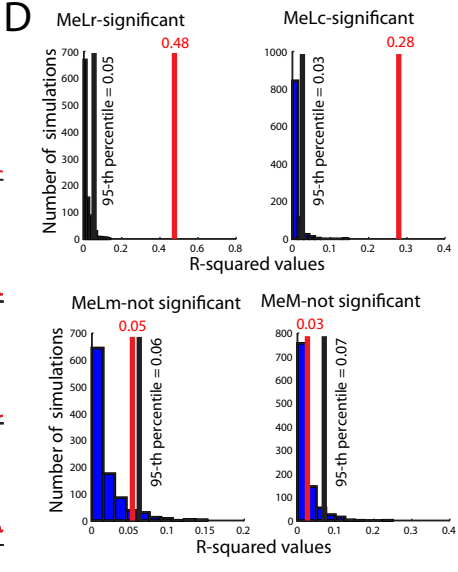

# SUPPLEMENTAL FIGURE 7

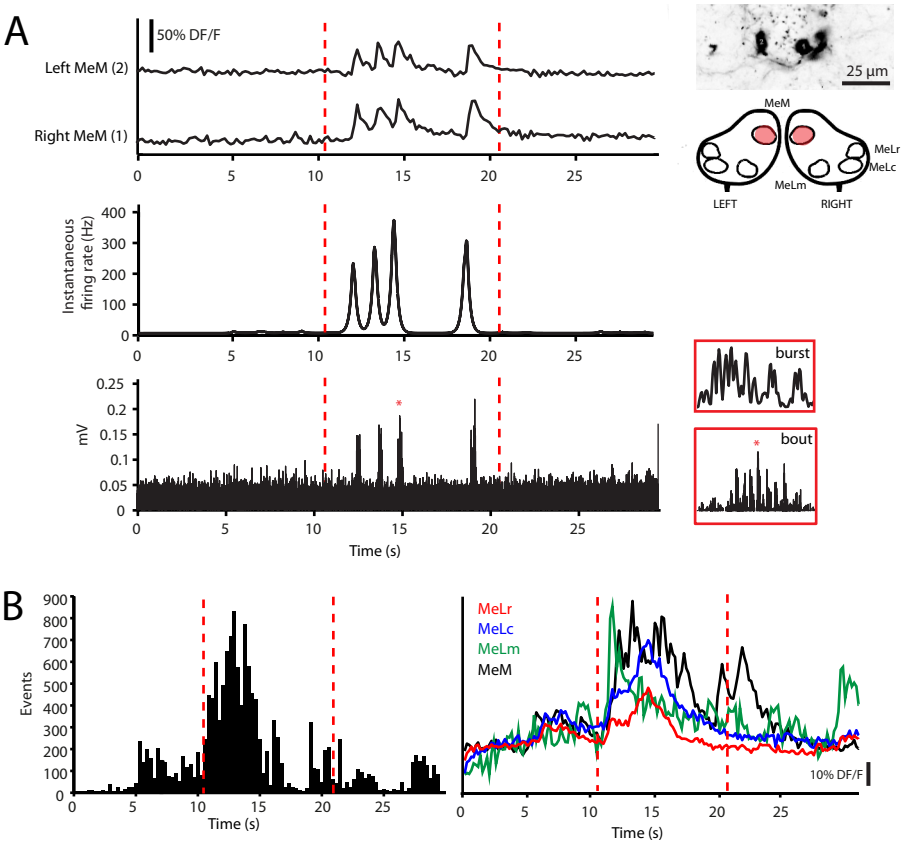

# SUPPLEMENTAL FIGURE 8

A

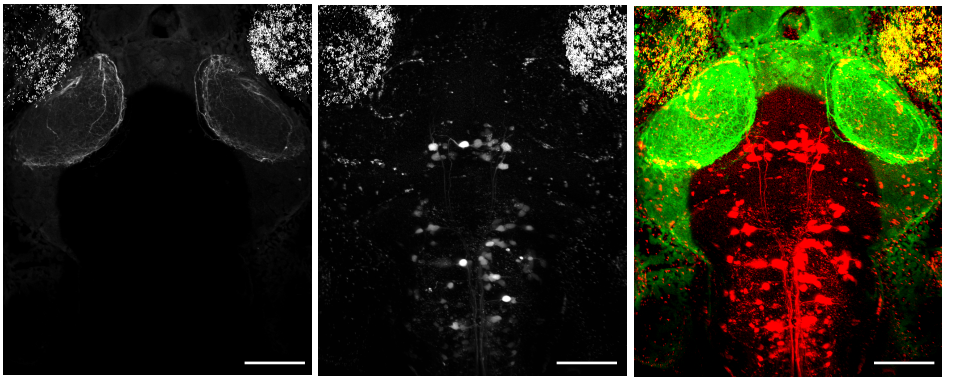

Ath5:Gal4; UAS:Dendra | Texas-Red Dextran backfill | Merge

B